

A Short-Circuit Experiment of High-Temperature Superconductor Tapes

Sataro Yamaguchi , Miho Eguchi , Shuhei Kawai , Masa Kanda , Yury Ivanov , Suzuo Saito, and Akira Ninomiya

Abstract—Superconducting dc power transmission (SCDC) is one of the most potent transmission lines because it is a low-loss, low-voltage, and small-cable system. However, one of the present technical issues is the short-circuit current. Since the current density of the high-temperature superconducting (HTS) tape is ~ 100 times higher than the copper and aluminum conductors in regular operation, it is more severe than the copper cables for the short-circuit current. We started the short-circuit experiments for a single HTS tape a few years ago. We constructed the capacitor bank to generate a short pulse current; its pulse duration is a few ms for the Bi2223 tape and ~ 60 ms for the RE123 tape. Their peak currents are 10 to 30 times larger than the critical currents (I_c) of the HTS tapes. We measure the I_c at the first step and flow the pulse current in the next step, and finally, we measure the I_c again if we can measure the I_c . If the I_c after the pulse current is lower than the original, the pulse current degrades the HTS tape. These are the ways of the experiments. We use RE123 tape; its initial I_c is 200 A, the pulse duration is ~ 60 ms, and the peak current is above 2.2 kA. After the pulse current, the I_c was almost identical to the original. However, if the peak current exceeded 2.4 kA, we observed the arc in the tape, and it broke the RE123 tape, or the critical current was lower than the original. We also tested the Bi2223 tape, which is more robust than the RE123 tape. At the same time, we estimated the temperature of the HTS tape during the discharge, which was higher than 300 degrees Celsius, even in liquid nitrogen (LN2), because the voltage-tap solder was molten. These experimental results are the basis for designing the HTS power cable.

Index Terms—Critical current, dc power cable, HTS tape, short circuit, temperature estimation.

I. INTRODUCTION

SUPERCONDUCTING dc power transmission (SCDC) is one of the most potent transmission lines because it is a low-loss, low-voltage, and small-cable system. The low voltage system is a crucial issue to connect with renewable energy (RE) power sources because the output power from the RE is not high, and their voltage system is usually lower than 30 kV. Therefore, the SCDC can connect them without high-voltage substations [1], [2]. Moreover, if the grid voltage is low, it is easy to use the semiconductor power devices, and therefore, its system has

Manuscript received 26 September 2023; revised 27 November 2023; accepted 22 December 2023. Date of publication 9 January 2024; date of current version 9 February 2024. (Corresponding author: Sataro Yamaguchi.)

The authors are with Chubu University, Kasugai, Aichi 487-8501, Japan (e-mail: yamax@isc.chubu.ac.jp).

Color versions of one or more figures in this article are available at <https://doi.org/10.1109/TASC.2024.3350017>.

Digital Object Identifier 10.1109/TASC.2024.3350017

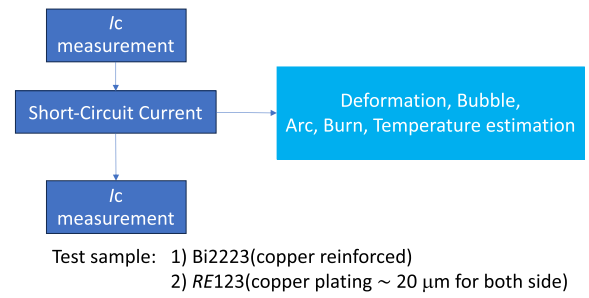


Fig. 1. Flow chart for the short-circuit experiment.

a high potential for flexible operation and is sometimes called an intelligent system or the smart grid [3], [4]. We can operate the grid system flexibly, and the total cost of the electric power system will be low.

However, one of the present technical issues is the short-circuit current. Since the current density of the high-temperature superconducting (HTS) tape is ~ 100 times higher than the copper and aluminum conductors, it would be more severe than the copper cables to protect from the short-circuit current. The short-circuit current is fixed for the present ac cable as one of the regulations in all countries [5], and some experiments have been done for the superconducting ac cable [6], [7], [8] along the present regulation. However, applying the same short-circuit condition may be severe for the superconducting ac cable because of the above reason, and the short-circuit condition will differ from the present regulation.

Furthermore, the regulation is flexible even for a dc copper cable because we connect power converters to the dc cable, and the short-circuit condition mainly depends on the power converter. Therefore, the short-circuit condition is fixed for individual systems. As a result, we started the short-circuit experiments for the HTS tape as the first step [9] a few years ago.

Fig. 1 shows the experimental flow chart to evaluate the HTS tape against the short-circuit current [10]. At first, we measured the critical current (I_c) of the HTS tape. Then, we perform the short-circuit current experiments of the HTS tapes and the high-current pulse applied to the HTS tapes. Since the peak current is higher than the I_c , the HTS tape is not superconducting when high current flows. The current density of the HTS tape would be several hundred times higher than the copper cable conductor.

Therefore, the HTS tape temperature in liquid nitrogen (LN2) will be higher than the melting point of the solder, even for

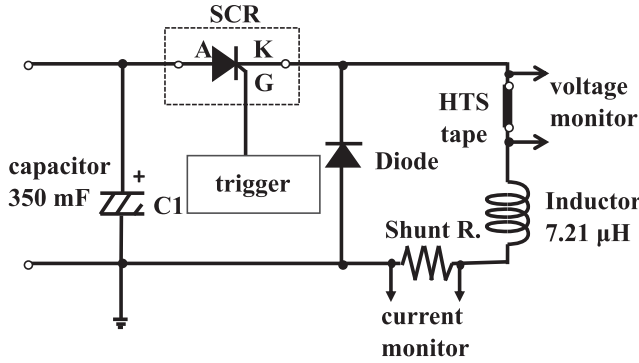


Fig. 2. Discharge circuit for the short-circuit experiment.

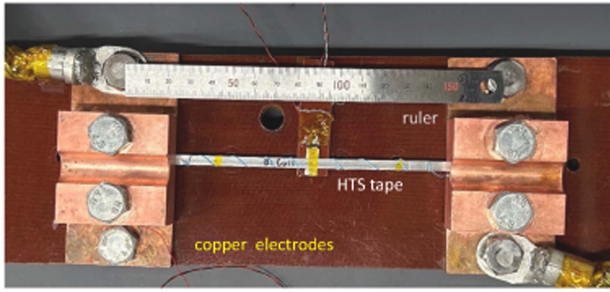


Fig. 3. Connecting electrodes and HTS tape on the board.

the short pulse duration. As a result, the HTS tape sometimes will be burned or deformed by thermal expansion. Therefore, temperature estimation is a critical issue in understanding the behavior of the HTS tape. After the short-circuit experiment, we measured the I_c of the HTS tape again to see if the HTS tape was not burned or destroyed. If the I_c is the same as the initial value, we can judge whether the HTS tape has durability for the short-circuit current.

We used two different kinds of HTS tapes for the experiment: the RE123 and the Bi2223 tapes. We compare their characteristics for the short-circuit experiment in the paper.

II. EXPERIMENTAL DEVICE AND PROCEDURE TO ESTIMATE TEMPERATURE DURING THE DISCHARGE

Fig. 2 shows the discharge circuit of the experiment [11]. The condenser capacitance is 350 mF, and we insert the inductor and the flywheel diode to make a long discharge. We used the SCR for the start switch and monitored the HTS tape voltage and the circuit current.

We connected the HTS tape to the copper electrodes, shown in Fig. 3, and the HTS tape surface touched LN₂ directly in the open cryogenic bath. We used the bolt and nut to connect the HTS tapes between the copper block, and the size of the bolt and nut is 12 mm. Before starting the experiment, we connected the HTS tape with the solder and compared the voltage and current waveforms. Fortunately, these waveforms are almost identical for solder and non-solder connections. We also did not observe the arc trace on the surfaces. Therefore, we did not use the solder connection in the experiment.

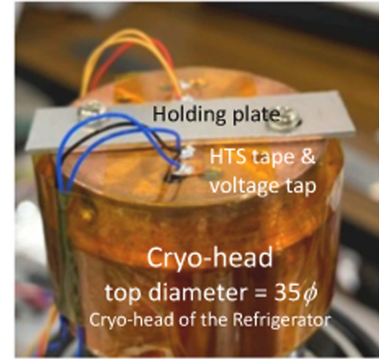


Fig. 4. Cryo-head photograph, amounting to the HTS tape, current and voltage taps, the holding plate, and cabling.

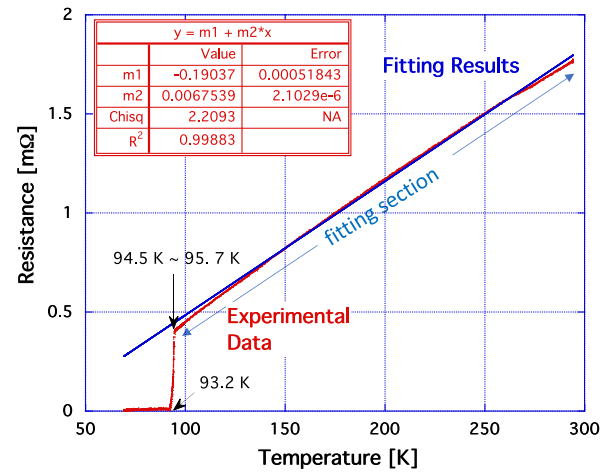


Fig. 5. Resistance measurement of the RE123 tape and its linear fitting result.

The length of the HTS tape is 150 mm, the voltage taps are connected by solder, and their distance is 100 mm.

We measured the HTS tape's resistance as the temperature's function. Fig. 4 shows the cryo-head of the refrigerator, amounting to the HTS tape, connecting with the voltage and current taps. We controlled the cryo-head's temperature and measured the HTS tape's resistance from room temperature (RT) to cryogenic temperatures. They were covered by multi-layer insulation (MLI) and set in a vacuum. Thus, we obtained the relations between the resistance and the temperature for the HTS tapes.

Fig. 5 shows the RE123 tape resistance from RT to the cryogenic temperature. The total thickness of the copper layers is 40 μm . We fitted the linear function for the normal state of the HTS tape. The critical temperature of the RE123 tape is 93.5 K \sim 94.5 K in the measurements, and the fitting result is quite good because the coefficient of determination R^2 is higher than 0.99. The fitting parameters' values and errors are shown in Fig. 5.

We estimate the resistance of the RE123 using the Handbook of Scientific Tables [12] for RT to 700 K, connecting with the experimental values. We also measured the resistance of the Bi2223 tape and performed the linear fitting the same as for the RE123 tape. Thus, we can estimate the temperature of the HTS tape during the discharge.

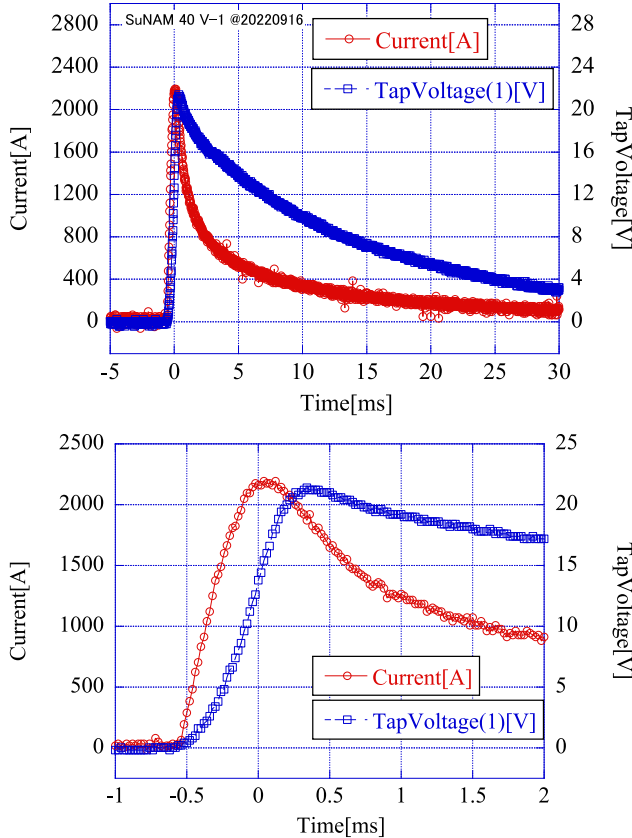


Fig. 6. Waveforms of the HTS tape voltage and the current for 40 V discharge; the upper figure shows the whole current and voltage, and the lower figure shows the beginning of the discharge.

III. EXPERIMENTAL RESULTS AND ANALYSIS FOR TEMPERATURE ESTIMATION

We used two HTS tapes in the experiment. One is the RE123 tape; it is lightweight, and its weight per length is 4.5 [g/m] because the copper stabilizer is as thin as 40 μm . The total thickness of the tape is 150 mm. The I_c is ~ 200 A. The other is the Bi2223 tape, whose weight per length is 13.0 [g/m]. The copper alloy stabilizer is 100 μm , the tape is a pure silver matrix, and the total thickness of the tape is ~ 350 μm . The I_c is ~ 190 A.

A. Experimental Result and Analysis of the RE123 Tape

Fig. 6 (upper) shows one of the whole waveforms of the HTS tape voltage (= tap voltage) and the current for RE123 tape, in which the charging voltage of the capacitor is 40 V. The lower figure shows the waveforms at the beginning of the discharge, and the growth rate of the current is nearly 4.0×10^6 A/s. The peak current is higher than 2200 A and more than 10 times higher than the I_c .

We can estimate the resistance R of the HTS tape during the discharge using (1), derived from the circuit equation.

$$R = \frac{1}{I} \left(V - L \frac{dI}{dt} \right) \approx \frac{V}{I} \quad (1)$$

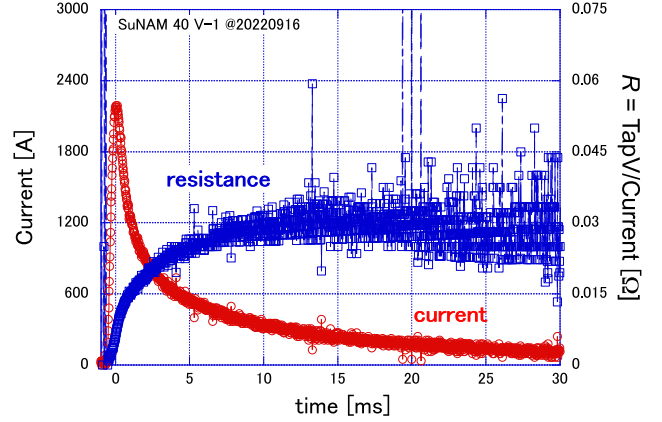


Fig. 7. Waveforms of the discharge current and the HTS tape voltage and current ratio.

where V is the tap voltage, I is the current, and L is the inductance of the HTS tape.

The inductance is calculated by the formula for the slab shape conductor [13], and its value is $0.8 \sim 1.0$ μH for the length of 100 mm, the thickness of $0.1 \sim 0.3$ mm, and the wideness of $4.0 \sim 4.5$ mm. Depending on the simple circuit analysis, the inductance voltage is smaller than the resistance voltage, and estimating the resistance from (1) is easy.

Fig. 7 shows the waveform of the current and the estimated resistance. The resistance values are calculated from the last term of (1). However, they are scattered in low-current value areas because of the experimental noises.

The resistance value is saturated to be $\sim 0.03 \Omega$ during the discharge time of 15 to 30 ms, and the correspondent temperature of the RE123 tape is ~ 600 K ($= 327$ degrees Celsius), estimated from Fig. 5 and the related discussions. Because of the high temperature, the voltage tap's solder melted, and the voltage tap was dropped off the tape surface, even in LN2.

We used the least-square-fitting method to avoid scattered data of the current and voltage, and we also included the inductance voltage to estimate the temperature of the RE123 tape during the discharge. Fig. 8 shows the fitting result for the resistance estimation.

The fitting functions are given by

$$V = mv1 + mv2 \cdot \text{Exp}[-mv3 \cdot t] \quad \text{for voltage} \quad (2)$$

$$I = m1 + m2 \cdot \text{Exp}[m3 \cdot (t + m4)] * \text{Sinh}[m5 \cdot (t + m4)] \quad \text{for current} \quad (3)$$

where $mv1$, $mv2$, $mv3$, $m1$, $m2$, $m3$, $m4$, $m5$ are the fitting parameters.

We estimate the real-time resistance of the HTS tape in the following way,

- 1) Getting the fitting parameters of the current and the voltage,
- 2) Differentiate the current and estimate the inductive voltage,

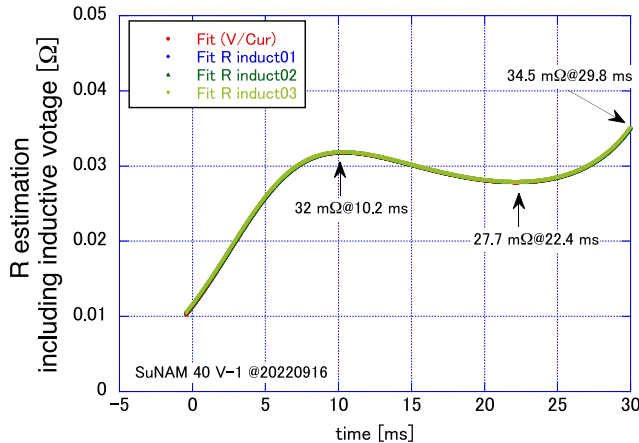


Fig. 8. Estimated the resistance of the RE123 tape by the least-square fitting, including the inductance voltage during the discharge.

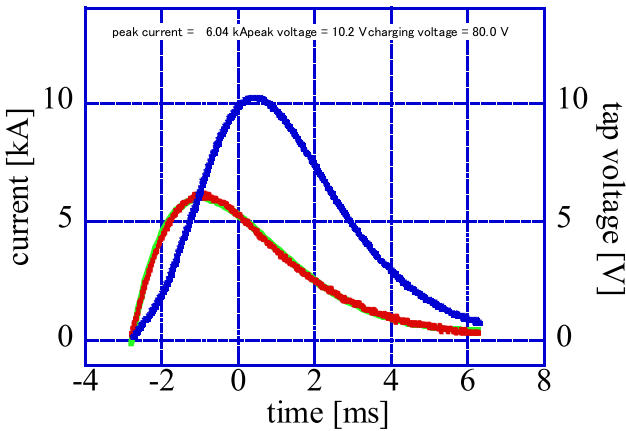


Fig. 9. Waveforms of the current and the voltage of the Bi2223 tape.

- 3) Take the difference between the observed fitting voltage and the inductive voltage, which is the resistive voltage,
- 4) Dividing the resistive voltage by the fitting current

Fig. 8 includes the inductance voltages, assuming the inductance of 0.0, 0.8, 0.9, and 1.0 μH . Since the inductive voltage is low, the resistance estimations are almost the same for the different inductances, and the resistance is $27 \text{ m}\Omega \sim 35 \text{ m}\Omega$ during the discharge. They correspond to temperatures of 590 K to 720 K. The fitting result is consistent with Fig. 7.

B. Experimental Result and Analysis of the Bi2223 Tape

We performed similar experiments for the Bi2223 tape. Fig. 9 shows the voltage and current waveforms, and the discharge start time was not zero because of the trigger level of the oscilloscope in this case. They include the waveforms of the fitting functions given by (3) for the current in the figure. The capacitor's initial voltage is 80.0 V, and the peak current is 6.04 kA. Since the I_c of the Bi2223 tape is $\sim 190 \text{ A}$, the peak current is ~ 30 times higher than that. The pulse length is shorter than the RE123 because the resistance is low. The tap voltage is lower than 10 V, less than half of Fig. 5, despite the peak current being three

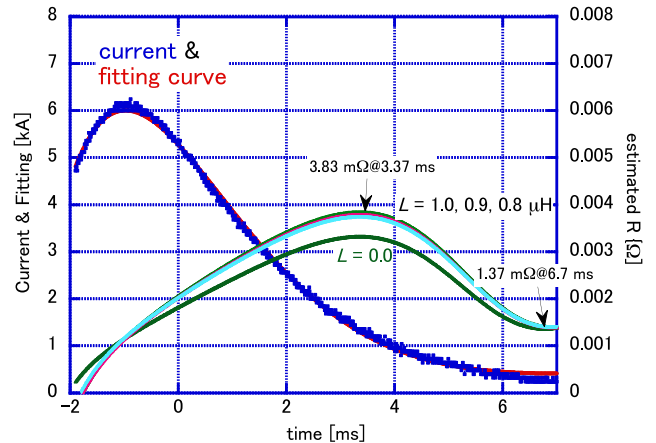


Fig. 10. Waveforms of the measured current and its fitting curve and the estimated resistance of the Bi2223 tape.

times higher than the RE123. The least-square fitting results are suitable for the current and the voltage, and the coefficient of determination R^2 is more elevated than 0.998. Therefore, the raw data plotting is almost identical to the fitting function curve. The waveform of the Bi2223 is shorter than that of the RE123 because the resistance of the Bi2223 tape is $\sim 1/10$ of the RE123 tape. Therefore, the temperature estimation should include the inductance voltage.

The discharge's start time depended on the oscilloscope's trigger level, and the current defines it as zero, and it is -2.78 ms in Fig. 8.

Fig. 10 shows the estimated resistance of the Bi2223 tape during the discharge, the raw current data, and the fitting curve of the current. If we include the inductive voltage, the resistance of the Bi2223 tape is low, and the peak resistance is $\sim 3.3 \text{ }\mu\text{W}$ around 3.4 ms. However, they are almost the same as $1.4 \text{ }\mu\text{W}$ around 7 ms in Fig. 10 because the time derivative of the current is close to zero.

The peak resistance is $\sim 3.8 \text{ m}\Omega$ around 3.8 ms, and down to $1.4 \text{ m}\Omega$ within 4 ms, and their correspondent temperatures are 620 K to 180 K. High-temperature time was short for the Bi2223 tape, and the solder remained to connect the voltage tap to the surface of the Bi2223 tape.

IV. DISCUSSION AND CONCLUSION

We made the present summary of the experiment for RE123 and Bi2223 in Table I. The solder of the voltage tap is melted for 40 V or higher voltage discharges for RE123 tape; the copper layer is 20 μm for both sides. The peak current of the short pulse is \sim ten times higher than the critical current (I_c) at $\sim 40 \text{ V}$ discharge of the capacitor. The estimated peak temperature of the tape is $\sim 600 \text{ K}$, and its duration is longer than 30 ms. This is why the voltage tap was dropped off the surface of the RE123. However, even if the solder is melted, the I_c is not down after the short-circuit experiments. Arc generation is not highly reproducible for the discharge voltage of 43 V, but when we observed the arc, the RE123 was broken down at the connection parts of the electrode. It is broken down depending on the thermal

TABLE I
EXPERIMENTAL SUMMARIES FOR RE123 TAPES

EXPERIMENTAL SUMMARIES FOR RE123 TAPES

Exp. No	Peak Current [kA]	Peak Resistance [$\text{m}\Omega$]	Estimated Peak Temp [K]	Comments
1	0.90	5.4	150	no degraded
2	1.17	9.9	250	↓
3	1.40	14.0	310	↓
4	1.62	20.0	444	↓
5	2.18	27.9	598	voltage tap left
6	2.21	32.0	575	↓
7	2.29	32.2	681	I_c down/ (arc)
8	2.37	45.9	943	arc + fracturing

EXPERIMENTAL SUMMARIES FOR Bi2223 TAPES

Exp. No	Peak Current [kA]	Peak Resistance [$\text{m}\Omega$]	Estimated Peak Temp [K]	Comments
9	4.68	2.1	272	no degraded
10	5.42	2.7	484	↓
11	6.04	3.8	618	↓
12	5.61	3.3	555	↓
13	6.75	5.2	748	I_c down, elongated
14	6.25	4.5	689	↓

expansion of the tape. However, the I_c is always down after the discharge voltage of 43 V. When the discharge voltage is 45 V, we consistently observed the arc generation, and the tape was broken at the connection parts. Therefore, the RE123 tape will be safe until the experimental condition's peak current is 1500 A or lower.

On the other hand, the Bi2223 tape is stronger for short-circuit current, and even if the peak current of the discharge is higher than 6000 A, the I_c was not down after the short-circuit discharge. However, the waveform is as short as ~ 6 ms for the same discharge circuit. The resistance of the Bi2223 tape is as low as 1/10 of the RE123s. Therefore, we cannot make a similar waveform of the RE123 for the same capacitor bank circuit, as shown in Fig. 1. The capacitance is simulated from the power converter circuit, and if we use a large capacitor, the current will be high. However, some power converter circuits do not use the output capacitor; the short-circuit current is suppressed, and we only consider the capacitance of the other parts of the circuit. We did not observe the arc generation in the Bi2223 tape experiment, but the estimated temperature was as high as ~ 700 K. Therefore, we should consider the thermal expansion of the Bi2223 tape. The length of the Bi2223 tape is a few mm longer than the initial length after the short-circuit experiment at RT. It is one piece of evidence that the estimated peak temperature of the Bi2223 tape is as high as 700 K. As a result, the Bi2223 tape was elongated after the experiment, and the critical current was down.

As mentioned, the HTS tapes' resistance is low for the Bi2223 tape. Therefore, we can make the copper layer thick for the RE123 tape; it can endure a high current pulse like the Bi2223

tape. If we can make the copper layer thick for the RE123 tape, the behavior of the RE123 will be similar to the Bi2223 tape. We will continue the short-circuit experiments for the HTS tape and prepare the short-circuit experiment for the cable as the next step.

The role of the authors;

The proposal was shown initially by S. Yamaguchi and discussed with all the authors at each step.

The experiments were done mainly by M. Eguchi and partially by S. Kawai, M. Kanda, S. Yamaguchi, Y. Ivanov, and A. Ninnomiya. M. Eguchi did the data gathering, and S. Yamaguchi did the analysis. All authors discuss the experimental and analytical results. S. Yamaguchi wrote the paper, and M. Kanda and Y. Ivanov edited it with S. Yamaguchi.

ACKNOWLEDGMENT

The authors would like to thank Mr. Takeshi Kihara for supporting experimental preparation at Chubu University, Japan, for his research activities.

REFERENCES

- [1] S. Yamaguchi, T. Yamada, T. Iitsuka, A. Sato, T. Sawamura, and V. Sytnikov, "Low voltage and large current dc superconducting power cable designs for 10 km to 100 km transmission line using experimental data of Ishikari project," *J. Phys.: Conf. Ser.*, vol. 1293, 2019, Art. no. 012067.
- [2] S. Yamaguchi, T. Iitsuka, T. Yamada, A. Sato, T. Sawamura, and V. Sytnikov, "Medium voltage cable designs for 100 km dc superconducting power transmission line using experimental data of Ishikari project," in *Proc. IEEE 3rd Int. Conf. dc Microgrids*, 2019, Matsue, Japan, pp. 1–4.
- [3] C. E. Bruzek, A. Allaix, D. Dickson, N. Lallouet, K. Allweins, and E. Marzahn, "Superconducting dc cables to improve the efficiency of electricity transmission and distribution networks: Overview," in *Eco-Friendly Innovations in Electricity Transmission and Distribution Networks*, J. L. Bessede, Ed. Cambridge, U.K.: Woodhead Pub., 2015, ch. 7, pp. 135–166.
- [4] H. A. Gabbar, A. M. Othman, A. Zidan, and M. Ahmed, "Operational design and control for smart medium-voltage direct current microgrids," in *Medium-Voltage Direct Current Grid: Resilient Operation, Control and Protection*, M. M. Eissa, Ed. London, U.K.: Academic, 2019, ch. 3, pp. 59–84.
- [5] *Japan Cable Standard (JCS) 0168-4:2010, 0501:2014*, Japanese Electrotechnical Committee. [Online]. Available: <https://jeea.or.jp/course/contents/04206/>
- [6] M. Ichikawa, T. Takahashi, H. Suzuki, S. Mukoyama, and M. Yagi, "Field tests of 500 M high-TC superconducting power cable and short circuit tests by short length cable," *J. Cryo. Soc. Jpn.*, vol. 41, no. 1, pp. 12–19, 2006.
- [7] T. Yasui et al., "Temperature and pressure simulation of a 1.5-km HTS power cable cooled by subcooled LN2 with a fault current," *IEEE Trans. Appl. Supercond.*, vol. 26, no. 3, Apr. 2016, Art. no. 5402005.
- [8] T. Masuda et al., "Test results of a 30 m HTS cable for Yokohama project," *IEEE Trans. Appl. Supercond.*, vol. 21, no. 3, pp. 1030–1033, Jun. 2011.
- [9] S. Yamaguchi, M. Kanda, and Y. Ivanov, "Short circuit-current experiment of the stacked conductor cable for aviation application," *CSJ Conf. Abstr.*, vol. 99, 2020, Art. no. 8.
- [10] S. Yamaguchi et al., "Short circuit-experiment of HTS tape conductor for superconducting dc power transmission (SCDC) - 4," *CSJ Conf. Abstr.*, vol. 105, 2023, Art. no. 104.
- [11] M. Eguchi et al., "Destructive and short-circuit current tests for high-temperature superconducting tape," in *Proc. Annu. Meet. IEEJ*, Mar. 202, pp. 5–144.
- [12] National Astronomical Observatory of Japan, "Chronological scientific tables, chapter of physics/chemistry," Maruzen-Yushodo Comp. Ltd., 2020.
- [13] H. Knoepfel, *Pulsed High Magn. Field*, Amsterdam, The Netherlands: North-Holland Publishing Comp., 1970.